

Near-IR Integral Field Spectroscopy with Adaptive Optics

N. Thatte, S. Anders, F. Eisenhauer, M. Tecza, S. Mengel, A. Eckart,
and R. Genzel

*Max-Planck-Institut für extraterrestrische Physik, Giessenbachstraße,
D-85748 Garching, Germany*

G. Monnet, and D. Bonaccini

*European Southern Observatory, Karl-Schwarzschild-straße 2, D-85748
Garching, Germany*

Abstract. Integral field spectroscopy, in conjunction with adaptive optics systems, has the unique potential of providing spectra at spatial resolutions close to the diffraction limit of the telescope. We present first results from integral field spectroscopy in conjunction with an adaptive optics system, achieving diffraction limited images and spectra at the Calar Alto 3.5 meter telescope. SINFONI, an adaptive optics assisted integral field spectrometer currently being built for the VLT, is one of the few adaptive optics optimized integral field instruments. We present a brief summary of its features, together with a brief description of the image slicer employed in SINFONI.

1. Introduction

Adaptive optics systems hold the promise of delivering diffraction limited images, allowing almost an order of magnitude gain in spatial resolution over that delivered by seeing. However, adaptive optics systems have mostly been used in conjunction with imaging devices (Hofmann et al. 1995, Rigaut et al. 1998, etc), although narrow band Fabry-Perot imagers have been employed with some systems (Chalabaev et al. 1999). Spectroscopy at resolutions close to the diffraction limit of the telescope holds immense promise of yielding fresh insights for a large range of astronomical problems. However, the difficulty of coupling spectrographs with adaptive optics systems has precluded their widespread use so far.

2. Spectroscopy at the diffraction limit

Three major difficulties stand in the way of adapting existing long slit spectrographs for use with adaptive optics systems.

- If the slit size employed by a long slit spectrograph is comparable to the diffraction limit of the telescope, then slit diffraction plays a dominant role in determining the point spread function (PSF) of the spectrograph.

Diffraction at the slit, located in a focal plane, results in a diffuse elliptical image of the telescope pupil. Any stop placed at this pupil image must either exclude a significant fraction of the light passing through the slit, or let in excess background emission (thermal or night sky) which would reduce the sensitivity of the instrument significantly.

- The light entering the spectrograph suffers diffraction at the slit, resulting in a smaller numerical value for the focal ratio than determined by geometrical optics. A spectrograph designed for large slit widths (when slit diffraction is unimportant) would suffer additional light loss due to vignetting by spectrograph optics and baffles.
- Adaptive optics systems typically deliver a PSF which consists of a diffraction limited core surrounded by a seeing limited halo. The relative amount of energy contained in the two components depends on a large number of factors, which include atmospheric seeing, guide star magnitude, angular separation of guide star and object, number of modes corrected, frequency of operation etc.. It is a common occurrence that the PSF varies on time scales of a few minutes, mostly due to variations in seeing and mechanical flexure of telescope components. Spectroscopy of extended objects needs information about the PSF, so that the various spatial contributions to the observed spectra can be identified and accurately estimated, even if no deconvolution is done. Since a long slit spectrograph only samples the PSF along one spatial direction (along the slit), it is impossible to recover sufficient information about the PSF to allow such analysis.

The first of these difficulties can be surmounted by including a pupil stop before the spectrograph slit. The stop (and succeeding optics) would need to be cooled if the instrument was cryogenic. The second problem may be overcome by over-designing the spectrograph optics, so as to include almost all the light diffracted by the slit, minimizing light loss. The third problem is more fundamental and may be overcome only by using a spectrograph which can recover two dimensional information of the PSF *during* the observation, namely, an integral field spectrometer. A Fabry-Perot spectroscopic imager may also be used, but the observer must then rely on the adaptive optics system to deliver a stable PSF during an entire scan covering the wavelength range of interest, which is rarely true in practice.

The OASIS spectrograph built for use with the PUEO adaptive optics bonnette of the CFHT (Bacon et al. 1999) is the first integral field spectrograph to be used in conjunction with an adaptive optics system. However, OASIS works at visible wavelengths, whereas adaptive optics systems deliver best performance in the near infrared. To exploit this unique area, we have mounted the MPE 3D near infrared integral field spectrometer at the focus of the ALFA adaptive optics system of the Calar Alto 3.5 meter telescope.

3. The AIM module

The MPE 3D integral field spectrometer (Weitzel et al. 1996) provides *simultaneous* spectra of 256 spatial pixels, arranged in a 16×16 square field of view on

the sky. Spectral resolutions of 1000 or 2000 are available, covering the H and K atmospheric windows. For further details of the 3D spectrograph, please refer to Weitzel et al. 1996. The ALFA laser star adaptive optics system (Hippler et al. 1998, Davies et al. 1998), is a collaborative effort of MPE and MPIA, operational since 1997 at the Cassegrain focus of the Calar Alto 3.5 meter telescope. ALFA's adaptive optics system is based on a Shack-Hartmann type wavefront sensor driving a deformable mirror with 97 actuators. Operating frequencies of upto 1200 Hz are possible, yielding closed loop bandwidths of ~ 120 Hz. A separate tip-tilt sensor allows operation with a laser guide star. The laser itself is a 3 Watt continuous wave laser operating at the frequency of the Na D line, producing an artificial star of $\sim 11^{\text{th}}$ magnitude at a height of about 90 km.

The MPE 3D integral field spectrometer was built to provide $0''.5$ pixels for the nominal $f/45$ focus of the Calar Alto telescope. To adapt the pixel scales of 3D for operation in combination with the ALFA adaptive optics system, the AIM (Aperture Interchange Module) interface has been designed (Anders et al. 1998). AIM performs four important functions.

- The pixel scale needed to correctly sample the diffraction limited images produced by ALFA is $0''.07$. However 3D's field of view (FOV) is always 16 times the pixel size in each linear dimension, so that choosing $0''.07$ per pixel yields a FOV of only $1''.1 \times 1''.1$. AIM allows on-the-fly scale changes between $0''.07$ and $0''.25$ per pixel, the latter corresponding to a $4'' \times 4''$ FOV.
- The AIM scale change optics include a small dewar with a Peltier cooled cold stop, which is inserted in the beam before the image slicer when the $0''.07$ pixel scale is chosen, thus avoiding any light loss or excess background due to slit diffraction effects.
- The small FOV implies that no pixels cover blank sky. In order to provide correct background subtraction, especially at near-IR wavelengths where the OH sky emission varies on time scales of a few minutes, AIM incorporates an ON-OFF mirror mechanism which allows 3D to observe two offset pointings within the ALFA FOV without moving the telescope. Using the ON-OFF feature, the time between successive 'nods' of the telescope can be increased from 2 minutes to 20 minutes, thus dramatically reducing the overhead needed to unlock and lock the adaptive optics system each time the telescope is pointed at blank sky. The 'chops' (on-offs) and 'nods' can be combined to yield a data set completely free of background flux from telescope and sky.
- AIM provides a set of pupil imaging optics which re-images the pupil of the adaptive optics system on the spectrograph image slicer. A reconstructed image of the 3D field may then be used to align the spectrograph pupil with that of the telescope and adaptive optics system, ensuring maximum throughput to the spectrograph.

Details of the construction of AIM can be found in Anders et al. 1998.

4. First results

We present first results from the commissioning run in August 1998, which used MPE 3D together with the ALFA adaptive optics system for the first time. Figure 1 shows a reconstructed image of the close binary HEI 7, which was observed with 3D + ALFA at a spectroscopic resolution of 2000 over the wavelength range 2.15 to 2.45 μm . The orbit of HEI 7 is well measured, with a separation between the primary and secondary components at the epoch of observations of $0''.26$ (Hershey 1975). The primary component has a visual magnitude $m_V = 7.1$, while the secondary component has $m_V = 10.0$. The spectral type of the primary is known to be K0 V, that of the secondary could only be estimated from colours to be M0 V. The reconstructed image of the PSF reference HD 183051, also $m_V = 7.1$, taken a few minutes prior to the observations of HEI 7, is shown on the left hand side of figure 1.

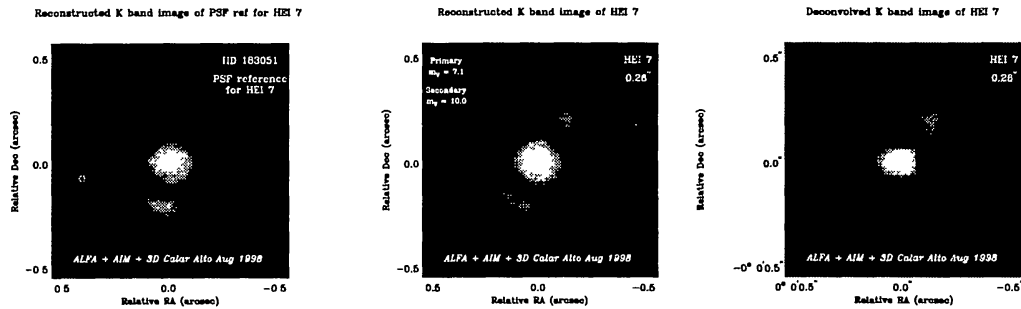


Figure 1. Reconstructed K band images of the binary star HEI 7 (central panel), the PSF reference star for HEI 7 (left panel) and the deconvolved data cube of HEI 7 (right panel). The images were made by collapsing the data cube in the spectral dimension. The PSF reference clearly shows a diffraction limited core ($0''.14$ FWHM), as well as part of the first Airy ring. The imperfect PSF of the adaptive optics system causes residual aberrations which distort the Airy pattern. The deconvolved image in the right hand panel shows the two components of the binary. The data cube also contains spectral information about each spatial pixel.

The image of the PSF reference clearly shows the need for two dimensional information of the PSF. Part of the first Airy ring around the diffraction limited core can be made out, but low order aberrations which cause flux to spill over into the first Airy ring can be easily seen. The PSF of the primary causes a $\sim 8.6\%$ contamination to the flux of the secondary.

The spectra extracted from a few pixels centered on the core of the primary and secondary components are presented in figure 2. The bottom part of the figure shows two spectra of template stars, taken from a library of near-IR stellar spectra, which have the same spectral types as those of the primary and secondary, the latter estimated from colours. As expected, the ^{12}CO bandheads (at 2.29, 2.32, 2.35 and 2.38 μm) are almost twice as deep in the secondary

compared to those in the primary, as are the Na ($2.21 \mu\text{m}$) and Ca ($2.26 \mu\text{m}$) absorption features. In contrast, the Mg feature (at $2.27 \mu\text{m}$) has the same depth in both the observed spectra as well as the templates. It should be noted the the signal-to-noise ratio of the spectra decreases dramatically toward the long wavelength edge of the K band, where thermal background emission from warm parts of the telescope and optics increases sharply.

The right hand panel of figure 1 shows a deconvolved reconstructed image of the binary star, created by deconvolving each plane of the data cube using the reconstructed image of the PSF reference star as the reference image. The deconvolution, though good, is not perfect, showing that even within a time span of a few minutes, and telescope inclination variations of a few degrees, the PSF delivered by the adaptive optics system varies substantially. In the case of the ALFA system, this dramatic variation in PSF is most probably caused by changes in flexure. In any case, these variations underpin the need to sample the PSF (in two dimensions) relatively frequently.

5. Future prospects

Several integral field instruments are planned for the 8 meter class telescopes which have recently been or will soon be put into operation. However, only a fraction of these integral field spectrographs plan to operate at near-IR wavelengths, and of those, only a fraction will be optimized for use with an adaptive optics system. In the following section, we report on SINFONI, the adaptive optics assisted integral field spectrometer for the ESO VLT.

5.1. SINFONI

SINFONI (Thatte et al 1998) is conceived from the start in the framework of a scientific collaboration between the Max-Planck-Institut für extraterrestrische Physik (MPE) and the European Southern Observatory (ESO) covering the field of high spatial resolution studies of compact objects (e.g. star forming regions, centers of galaxies, cosmologically distant galaxies). SINFONI is a combination of two instruments, a near-infrared integral field spectrometer, SPIFFI II (Tecza et al. 1998), and a curvature sensor based adaptive optics system MACAO (Bonaccini et al. 1998).

The near infrared integral field spectrometer, SPIFFI II, which is the responsibility of the MPE group, obtains 1024 simultaneous spectra covering a 32×32 contiguous square field of view, with a filling factor close to 100%. The pixel size may be chosen to be $0''.25$ per pixel for seeing limited observations, or $0''.03$ per pixel for diffraction limited observations, or $0''.1$ for intermediate observing conditions. The corresponding fields of view are $8'' \times 8''$, $1'' \times 1''$, and $3''.2 \times 3''.2$ respectively. Four different gratings are available, providing spectral resolutions of ~ 4500 covering one of the J, H or K bands, or both H and K bands simultaneously at a spectral resolution of 2000. The high spectral resolution settings would allow an *OH avoidance* technique to be implemented. Since 98% of the night sky emission flux in the wavelength range from 1.0 to $2.2 \mu\text{m}$ is contained in OH lines, a substantial reduction in sky background flux may be achieved by simply blanking out those pixels in the spectrum which are contaminated by OH line emission.

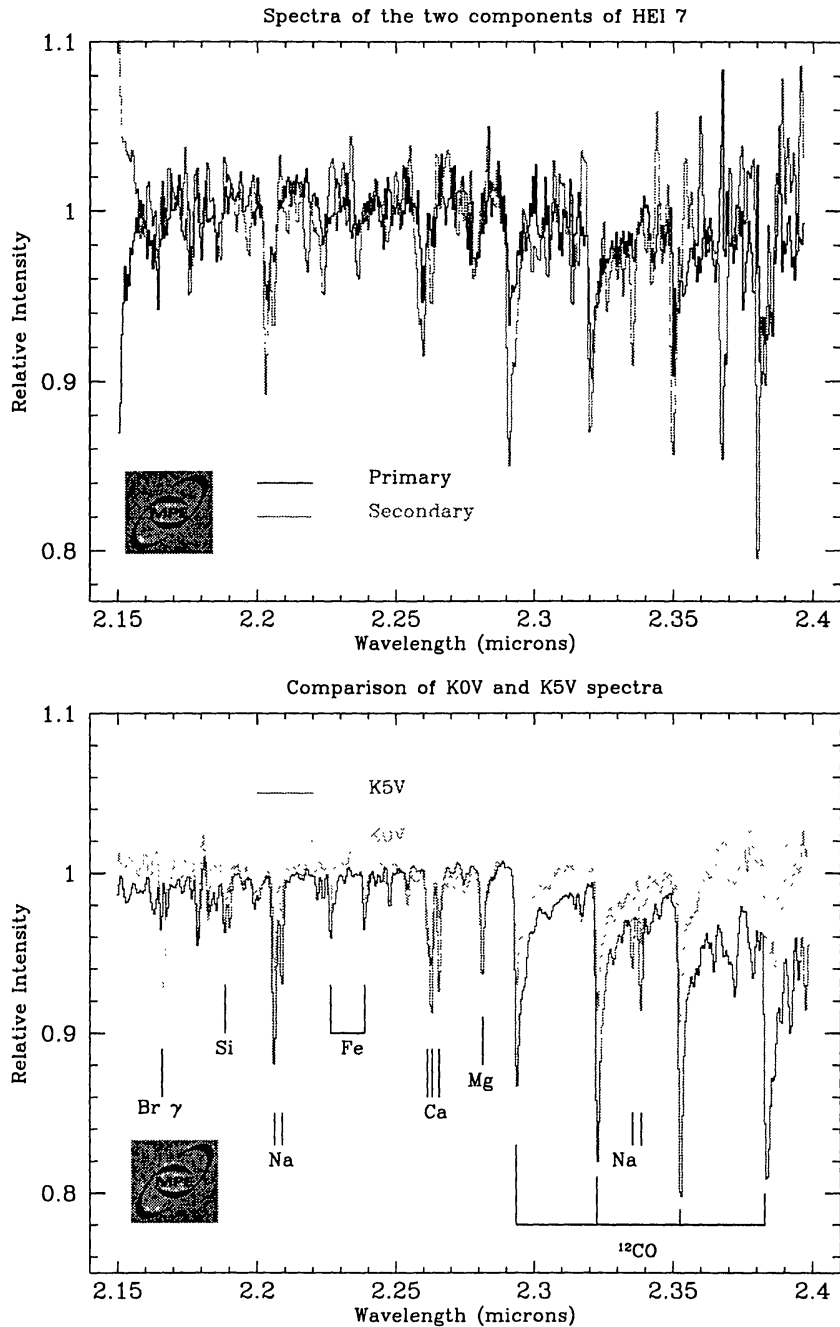


Figure 2. Spectra of the two components of HEI 7 are shown in the top panel for the long wavelength half of the K band. Two spectra of template stars from a stellar library are illustrated in the bottom panel for comparison. The spectral types of the template stars are chosen to match those of HEI 7. The spectrum of HEI 7 suffers from enhanced noise longward of 2.3 μ m, due to thermal background from telescope and warm optics. The CO bandhead at 2.29 μ m is twice as deep in the secondary as in the primary, while the Mg feature at 2.27 μ m has the same depth in the two stars, as expected.

In addition, SPIFFI II incorporates a *Himmelspinne*, which allows light from one of four pre-selected offset positions to be redirected to the image slicer, and then onto the detector. This precludes the need to nod the telescope every couple of minutes in order to measure the variable sky background accurately. Combined with the OH avoidance capability, this would allow integrations of roughly 1 hour duration. An imaging channel with $25'' \times 25''$ FOV is available, in order to ease acquisition of faint targets. A pupil imaging system is also included, so as to ensure accurate alignment of the telescope and adaptive optics system pupils with that of the spectrometer.

The curvature sensor based adaptive optics system MACAO (Bonaccini et al. 1998), which is the responsibility of ESO, incorporates a deformable mirror with 67 actuators. It uses photon counting Avalanche Photodiodes (APDs) for wavefront sensing, providing extremely high sensitivity. The system is specifically optimized to provide low order correction using very faint guide stars. Its performance is well adapted to spectroscopic applications, where energy concentration is more important than achieving diffraction limited image quality. MACAO can use a guide star within a field of $2'$ diameter centered on the scientific target. Its novel design implies only three warm reflections (apart from the primary and secondary) before the light enters the cryogenic spectrometer. The dewar window itself serves as the dichroic, reflecting the visible light to the wavefront sensor. The extra thermal background added by the relay optics is thus kept to an absolute minimum, dramatically improving the sensitivity of SINFONI in the K band, where thermal emission from warm telescope optics and surroundings can dominate the background flux seen by the spectrometer. MACAO can also be used with a laser guide star, which is foreseen to be a standard facility for the VLT ANTU (formerly UT1) telescope.

5.2. The SINFONI Image Slicer

The heart of SPIFFI II is the image slicer, which rearranges the light from a two dimensional field on the sky to a (pseudo) long slit feeding the spectrograph collimator. Figure 3 shows the conceptual design of the SPIFFI II image slicer, which is based on the image slicer employed in the MPE 3D spectrograph. The slicer consists of two stacks of plane mirrors, dubbed the *small slicer* and *big slicer*. The stack of small slicer mirrors resembles a spiral staircase. It is composed of gold coated mirrors, each 9.6 mm long, but only 0.3 mm thick. Each mirror has a different tilt to the incoming light path, and redirects the light to a particular mirror segment of the big slicer.

The big slicer consists of 32 segments, one for each of the small slicer mirrors, whose midpoints are located on a parabola. The small slicer sits at the focus of the parabola. In addition, the big slicer mirrors are arranged in two layers, forming a brick-wall pattern, with 16 segments in each layer. Each big slicer mirror redirects the light from the corresponding small slicer mirror so that it is parallel to the incoming beam. The image slicer thus preserves the pupil position, which is set to infinity for the entrance pupil. The brick-wall arrangement of big slicer mirrors allows each mirror to be almost twice as long as the nominal slitlet length it re-images, thus avoiding any light loss due to defocus effects.

The total re-imaged slit length is 307.2 mm, and is composed of 32 slitlets, each 9.6 mm long. Each slitlet is in turn imaged onto 32 detector pixels, thus

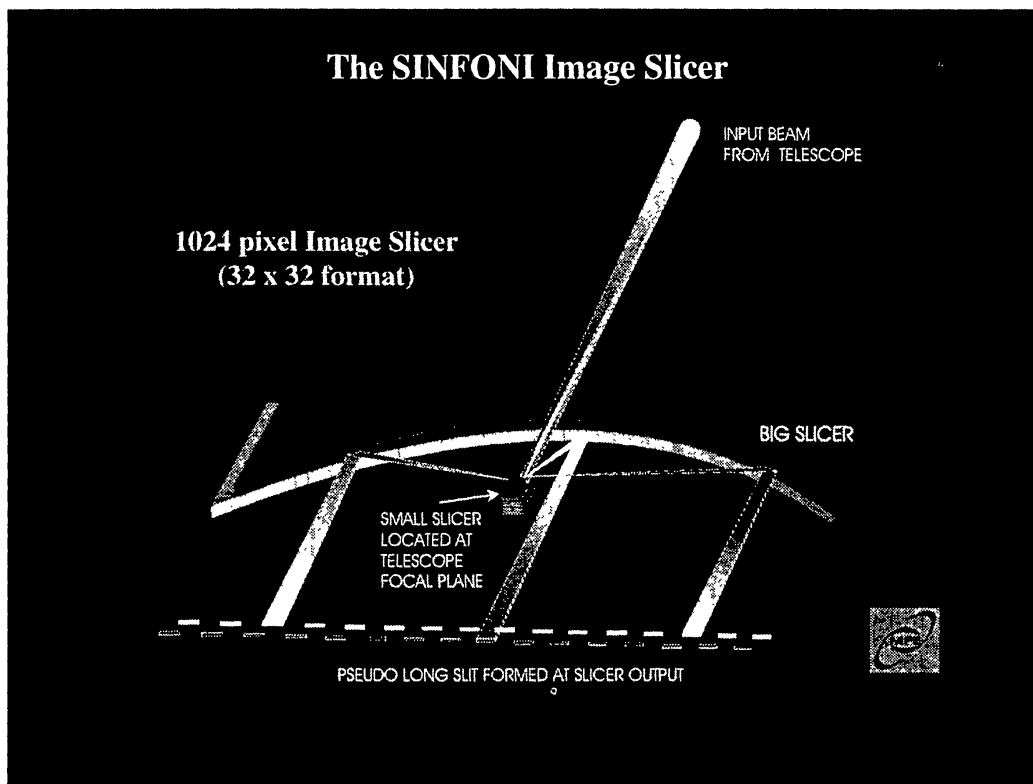


Figure 3. Conceptual design of the SPIFFI II image slicer. The incoming beam (with entrance pupil at infinity) is incident on a stack of plane mirrors (small slicer) which redirect the light in different directions depending on its height in the image plane. The second stack of plane mirrors (big slicer) then redirects the light from each slice (or slitlet) so that it is parallel to the incoming beam (pupil preserving). The big slicer mirrors form a two level brick-wall pattern. Their centers are located on a parabola, whose directrix is the location of the virtual slit.

providing 1024 spectra covering a 32×32 square field of view. The re-imaged slit is virtual, and is located behind the big slicer mirrors, along the directrix of the parabola which defines the positions of the big slicer mirrors. The computed throughput of the SPIFFI II slicer has an average value of 89%, degrading slowly from the center to the edge of the field along each slitlet. The entire slicer is cooled to the instrument's operating temperature of 77 K. The individual slices of the small slicer are optically contacted to each other, thus avoiding any glue (which could lead to misalignments and non-reflecting zones) and extremely high image quality over the whole field.

5.3. Alternative Slicer Concept

We are also pursuing an alternative concept for the SPIFFI II image slicer, using OH free silica-silica fibers to do the image slicing. These fibers show adequate transmission ($\geq 90\%$) out to the long wavelength edge of the K band ($2.5 \mu\text{m}$), if short lengths ($\sim 15 \text{ cm}$) are used. They are much more robust than "infrared fibers" (e.g. ZrF) and standard handling and polishing techniques may be used. Optical fibers have been used for image slicing for a long time at visible wavelengths (Arribas et al. 1998). There are typically combined with an array of lenslets so as to provide good filling factor in the image plane (Kenworthy, Parry and Taylor 1998). The lenslets form tiny images of the telescope pupil matched to the diameter of the fiber core. However, the difficulty of maintaining the alignment between lenslets and fibers at cryogenic temperatures has precluded their use in infrared instruments.

The *flared fiber* concept (Tecza and Thatte 1998) circumvents the cryogenic alignment problem by combining the microlens and the fiber into a single monolithic unit. The fiber end is heated and "flared", in a process akin to the reverse of drawing the fiber. The flared tip is then ground, so as to remove the cladding material, leaving bare core material in the shape of a "taper". The front surface of this taper is then polished to form a lenslet with the required radius of curvature, and the sides are ground to form a regular hexagon. One such flared fiber is shown in the left hand panel of figure 4. These individual units can then be arranged in a close packed geometry to form the image slicer, as illustrated in the right hand panel of figure 4. Since each fiber and its microlens are part of the same monolithic unit, relative alignment is maintained even when the whole unit is cooled to cryogenic temperatures.

The other ends of the fibers are all arranged to lie along a straight line, forming the entrance slit of the cryogenic spectrograph. This concept has the advantage that it is easily expandable to a large number of image points (fibers). Small bundles may also be used to form *deployable IFUs*, which could be placed by a cryogenic robot within a large field of view. Our preliminary tests of this concept have been very encouraging, yielding fibers with $>80\%$ coupling efficiency. We will pursue this concept further, for use in future instruments.

We would like to acknowledge the tremendous effort of the ALFA + 3D team, in particular, R. Davies, W. Hackenberg, S. Hippler, M. Kasper, T. Ott, S. Rabien and R. Sosa-Brito during the ALFA + 3D run in July-August 1998. We also thank the MPE staff for their help in building instruments and interfaces. We are grateful to the Calar Alto staff for their help at the telescope.

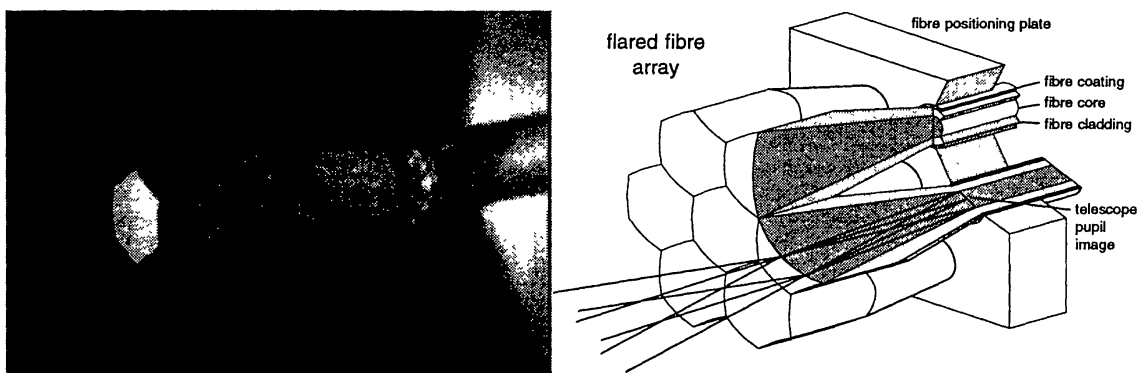


Figure 4. Photograph of a single flared fiber is shown in the left hand panel. The hexagonal lenslet has a size of $600\ \mu\text{m}$. The unflared part of the fiber is held in a metal ferrule to protect it during the polishing process. The right hand panel illustrates the concept of an image slicer built using flared fibers. Each lenslet forms an image of the telescope pupil on to the fiber core. The numerical aperture of the fiber is chosen to match the focal ratio of light from the lenslet.

References

- Anders, S., Maiolino, R., Thatte, N., and Genzel, R. 1998, Proc. SPIE, 3354, 222
- Arribas, S. et al. 1998, Proc. SPIE, 3355, 821
- Bacon, R. et al. 1999, in press
- Bonaccini, D., Rigaut, F., Dudziak, G., and Monnet, G. 1998, Proc. SPIE, 3353, 553
- Chalabaev, A., le Coarer, E., Rabou, P., Magnart, Y., Petmezakis, P., and Le Mignant, D. 1999, Proc. of ESO/OSA meeting "Astronomy with Adaptive Optics", Sonthofen, Germany, in press
- Davies, R. et al. 1998, Proc. SPIE, 3353, 116
- Hershey, J. 1975, AJ, 80, 662
- Hippler, S. et al. 1998, Proc. SPIE, 3353, 44
- Hofmann, R., Brandl, B., Eckart, A., Eisenhauer, F., and Tacconi-Garman, L. E. 1995, Proc. SPIE, 2475, 192
- Kenworthy, M., Parry, I., and Taylor, K. 1998, Proc. SPIE, 3355, 926
- Rigaut, F. et al. 1998, PASP, 110, 152
- Tecza, M. and Thatte, N. 1998, in "Fiber Optics in Astronomy III", ASP Conference Series, 152, 271
- Tecza, M., Thatte, N., Krabbe, A., and Tacconi-Garman, L. E. 1998, Proc. SPIE, 3354, 394
- Thatte, N. et al. 1998, Proc. SPIE, 3353, 704
- Weitzel, L., Krabbe, A., Kroker, H., Thatte, N., Tacconi-Garman, L. E., Cameron, M., and Genzel, R. 1996, A&AS, 116, 531